Cationic UV Curing Behavior and Thermal Properties of Oxetane-Modified Polysiloxane Prepared from Tetraethyl Orthosilicate

Fu Zhan, Xi-e Cheng, Wenfang Shi

CAS Key Laboratory of Soft Matter Chemistry, Department of Polymer Science and Engineering, University of Science and Technology of China, Hefei, Anhui 230026, People's Republic of China

Received 16 January 2011; accepted 10 March 2011
DOI 10.1002/app.34497
Published online 2 August 2011 in Wiley Online Library (wileyonlinelibrary.com).

ABSTRACT: The oxetane-modified polysiloxane (Oxe-PSiO) was synthesized via the partial hydrolysis/condensation of tetraethyl orthosilicate (TEOS) and then transesterification reaction with 3-ethyl-3-(hydroxymethyl)oxetane (EHO), and characterized by FT-IR, ^{1}H NMR, ^{13}C NMR, and ^{29}Si NMR spectroscopy. Using the water/TEOS molar ratios of 0.8–1.2, the number-average molecular weights and polydispersity indices were obtained by GPC to range from 1.013 to 2.716 g mol^{-1} and around 2.0, respectively. The viscosity of Oxe-PSiO prepared from the water/TEOS molar ratio of 1.2 sharply increased to 177,545 cps from 438 cps of that from the molar ratio of 0.8. A series of cationic UV-curable formulations were prepared by blending the Oxe-PSiO synthesized with the water/TEOS molar ratio of 1.0 into an commercial oxetane-based resin, 3,3′-[oxydi(methylene)]bis(3-ethyloxetane), in different weight ratios. The photopolymerization kinetics studied by photo-DSC in the presence of triphenylsulphonium hexafluoroantimonate as a cationic photoinitiator showed that both the maximum photopolymerization rate and final oxetane conversion in the cured film decreased with increasing Oxe-PSiO loading mainly due to the sharp increase in viscosity. The DMTA and DSC results both indicated the improvement in thermal stability, showing 12 and 13.4°C, respectively, higher T_g for the cured film with 50 wt % Oxe-PSiO loading compared with the pure polymer. Moreover, the temperatures ($T_{10\%}$ and $T_{50\%}$) at the weight loss of 10 and 50% and final char yields measured by TGA increased with increasing Oxe-PSiO content. After adding 50 wt % Oxe-PSiO, compared with the pure polymer the $T_{10\%}$ increased from 349 to 361°C, while the $T_{50\%}$ increased from 409 to 424°C, and with a char yield increase of 8.2% at 800°C. In addition, its greatly increased crosslinking density due to the formation of silica network resulted in the enhancement in pencil hardness from B of the pure polymer to 2H grade. © 2011 Wiley Periodicals, Inc. J Appl Polym Sci 123: 717–724, 2012

Key words: oxetane; polysiloxanes; cationic UV curing; photopolymerization; coating

INTRODUCTION

Polysiloxanes have been widely used as important coating materials in various fields.[1–3] They mainly consist of Si—O bond which has high bond dissociation energy of 451 kJ mol^{-1} compared with 347 kJ mol^{-1} for C—C, 359 kJ mol^{-1} for C—O, and 326 kJ mol^{-1} for Si—C.[4] Thus polysiloxanes exhibit some special chemical and physical properties, especially such as weatherability, thermal stability, and chemical resistance. Many polysiloxanes have been developed to improve coating performance through cold blend or chemical modification.[5–7] As a well-accepted and environment-friendly technology in coating area,[8–13] the UV curing has also attracted great attention in the application of polysiloxanes. One important approach for synthesis of UV curable polysiloxanes is hydrolysis and condensation of organoalkoxysilanes $R'Si(OR)_3$, where R' is a UV curable functional group via radical or cationic means.[14–17]

In contrast to free radical UV curing systems, cationic UV systems exhibit some advantages, such as better adhesion, low shrinkage, low toxicity, and absence of oxygen inhibition.[18–20] Two organoalkoxysilane monomers, 3-glycidoxypropyl-trimethoxysilane (GPTMS) and 2-(3,4-epoxy-cyclohexylethyl)ethyltrimethoxysilane (TRIMO), have attracted considerable interest for preparing cationic UV curable polysiloxanes.[21,22] However, both the hydrolysis and condensation of organoalkoxysilane are very slow in the absence of a catalyst. On the one hand, the basic catalyst such as amines should not be used as it probably neutralizes the Lewis acid produced by cationic photoinitiator and inhibits the cationic curing. On the other hand, the acid catalyst may result in the ring opening reaction of epoxy group in GPTMS or TRIMO and cause gelation during the synthesis procedure or storage stage. Thus the condition for

Correspondence to: W. Shi (wfshi@ustc.edu).
Contract grant sponsor: National Natural Science Foundation of China; contract grant number: 50973100.

preparing cationic UV curable polysiloxane should be well controlled compared with that for preparing radical one. Crivello and coworkers synthesized a series of polysiloxanes with a weakly acid ion exchange resin so as to catalyze the inorganic polymerization of epoxy-containing organoalkoxysilane. The ion exchange resin as an acid catalyst can be removed by simple filtration. The final polysiloxanes-bearing epoxy groups can undergo facile UV curing in the presence of a cationic photoinitiator.[23,24]

However, so far, most researches focus on epoxy-based cationic UV curable polysiloxanes. The oxetane-based ones, which may possess high reactivity due to their high nucleophilicity and strong ring strain,[25–27] were seldom reported. This is probably due to the lack of commercial and commonly used organoalkoxysilanes containing oxetane group. In this work, the oxetane-modified polysiloxane (Oxe-PSiO) was synthesized via partial hydrolysis and condensation of tetraethyl orthosilicate, and then transetherification reaction with 3-ethyl-3-(hydroxymethyl)oxetane. The molecular structures were characterized by FT-IR, ^{1}H NMR, ^{13}C NMR, and ^{29}Si NMR spectroscopy. The effects of molar ratio of water to TEOS on the molecular weight and viscosity were investigated. The Oxe-PSiO was added into a commercial oxetane-based resin with different ratios to prepare a series of cationic UV curable formulations. The photopolymerization kinetics was characterized by using photo-DSC method. The viscoelastic, physical properties and thermal degradation performance of UV cured films were also investigated by DMTA, DSC, and TGA, respectively.

EXPERIMENTAL

Materials

The 3-ethyl-3-(hydroxymethyl)oxetane (EHO) was supplied by Perstorp AB, Sweden. Tetraethyl orthosilicate was supplied by Shanghai First Reagent, China. Titanium tetraisopropanolate was supplied by Daoning Chemical, Nanjing, China. Triphenylsulphonium hexafluoroantimonate used as a cationic photoinitiator, and a commercial oxetane-based cationic resin, 3,3′-[oxydi(methylene)]bis(3-ethyloxetane) (DOX), were supplied by Ginray Chemical, Shanghai, China. Other chemicals were purchased from Shanghai First Reagent, China. All the chemicals were used as received without further purification except for EHO, which was dried with 4-Å molecular sieves before use.

Measurements

The Fourier transfer infrared (FT-IR) spectra were recorded with a MAGNA-IR 750 spectrometer (Nicolet Instrument, USA). The ^{1}H NMR and ^{13}C NMR, and ^{29}Si NMR spectrum were recorded with a Bruker 300-MHz instrument, and a Bruker 400-MHz instrument, respectively, using $CDCl_3$ as a solvent. The number-average molecular weight and its polydispersity index were determined with a gel permeation chromatography (GPC) equipped with a refractive-index detector, and calibrated with the standard linear PSt. THF was used as an eluent with a rate of 1.0 mL min^{-1}. The viscosity at room temperature was measured with a TA Instrument AR-G2 rheometer.

The photopolymerization kinetics was monitored by using a TA Q2000 differential scanning calorimeter (DSC) equipped with a UV spotcure system (Qmnicure series 2000). About 2 mg homogeneous formulation was weighted into the aluminum pan, and then exposed under the UV spotcure system in N_2 atmosphere. The incident light intensity at the sample pan was measured to be 150 mW cm^{-2} using a UV powermeter. The oxetane conversion in the cured film (P_t) was calculated by the formula, $P_t = H_t/H_\infty$, where H_t is the heat released within t s, H_∞ is the heat release of 100% oxetane group conversion. The DSC curves were unified by the weight (g) of sample. The polymerization rate is defined by J g^{-1} s^{-1}, namely, the heat release of polymerization per second for 1 g samples. For calculating the polymerization rate and H_∞, the value $\Delta H_0 = 107$ J mmol^{-1} was taken for the heat release of polymerization per oxetane group.

The differential scanning calorimetry (DSC) curves were recorded with a TA Q2000 apparatus. All the samples were heated from −20 to 150°C with a rate of 10°C min^{-1} in N_2 atmosphere for the first scan, then cooled to −20°C at 10°C min^{-1}, and immediately heated at 10°C min^{-1} from −20 to 150°C again.

The tensile storage modulus (E') and tensile loss factor (tan δ) were measured using a dynamic mechanical thermal analyzer (Diamond DMA, PE) at a frequency of 2 Hz and a heating rate of 10°C min^{-1} in the range of −50–160°C on the sheet of 25 mm × 5 mm × 1 mm. The thermogravimetric analysis (TGA) was carried out by using a TGA Q5000 instrument in the range from 30 to 800°C with a heating rate of 10°C min^{-1} in N_2 atmosphere. The pencil hardness of the cured films was determined using a QHQ-A pencil hardness apparatus (Tianjin Instrument, China).

Synthesis

A typical procedure for synthesizing the oxetane-modified polysiloxane (Oxe-PSiO) with the same molar amount of water and TEOS is given as follows: a mixture of TEOS (40.67 g, 0.2 mol) and acidified water (3.60 g, 0.2 mol, containing 0.2 × 10^{-3} mol HCl) was poured into a glass flask equipped with a mechanical stirrer, gas-inlet and -outlet tube,

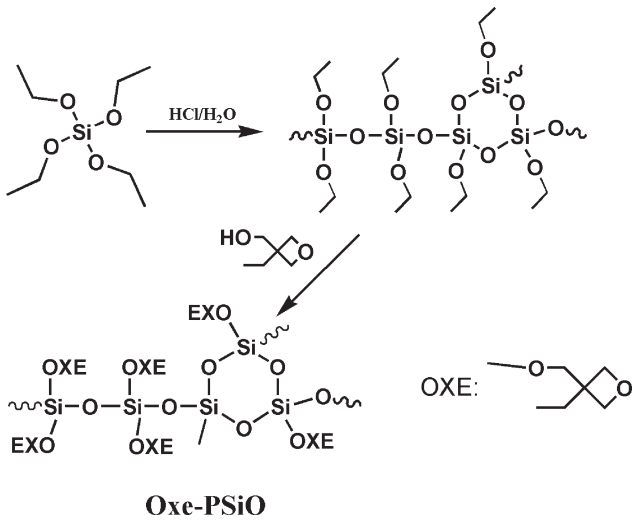

Scheme 1 Synthetic route of Oxe-PSiO.

and reacted at room temperature for 1 h, at 80°C for 10 h and at 150°C for 3 h. N_2 was pumped into the reactant to exclude the ethanol formed during the condensation. After the reaction temperature was decreased to 120°C, EHO (51.11 g, 0.44 mol) and titanium tetraisopropanolate (0.11 g, 0.4×10^{-3} mol) were charged into the flask, and stirred continuously under N_2 flow until the ^{1}H NMR signal peak at 1.23 ppm for CH_3CH_2O—Si disappeared completely. Finally, the superfluous EHO was removed from the reactant under reduced pressure. The Oxe-PSiO was obtained as a pale yellow liquid.

^{1}H NMR (300 MHz, $CDCl_3$): δ (ppm) 4.5–4.3 (oxetane—*H*), 4.0–3.9 (oxetane—CH_2—O—Si), 1.8–1.6 (CH_3—CH_2—oxetane), 1.0–0.8 (CH_3—CH_2—).

^{13}C NMR (300 MHz, CDCl3): δ (ppm) 79–77 (oxetane—*C*), 67–65 (oxetane—CH_2—O—Si), 44–43 (CH_3—CH_2—*C*), 26–25 (CH_3—CH_2—), 8–7 (CH_3—CH_2—).

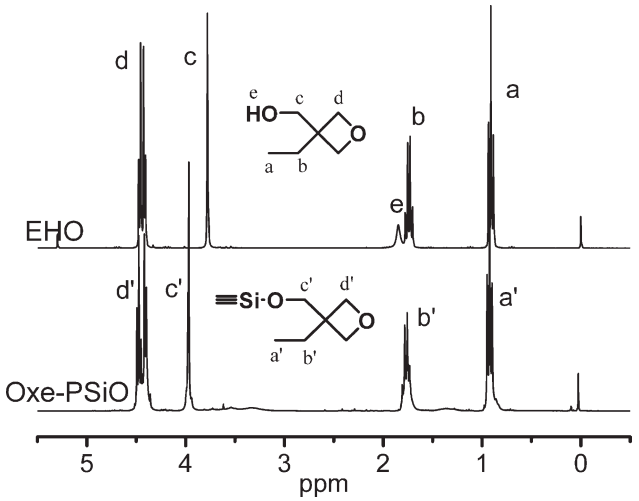

Figure 1 ^{1}H NMR spectra of EHO and Oxe-PSiO.

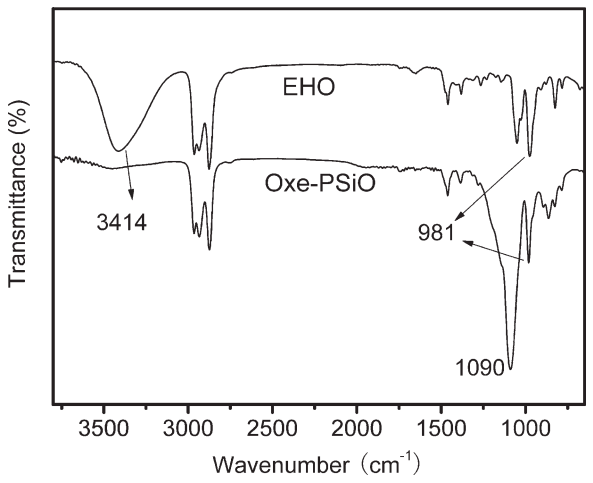

Figure 2 FT-IR spectra of EHO and Oxe-PSiO.

Sample preparation

A mixture of DOX as a prepolymer and EHO as a dilute monomer with a weight ratio of 6 : 4 was selected as a matrix resin and named as DE. The formulations containing different ratios of DE to Oxe-PSiO were prepared with the addition of 2 wt % triphenylsulphonium hexafluoroantimonate as a cationic photoinitiator, and then exposed to a medium pressure mercury lamp (2 KW, Fusion UV systems, USA) for 2 min to obtain the cured films, which denoted as DE_mPSiO_n, where *m* is the percentage of DE, and *n* is the percentage of Oxe-PSiO.

RESULTS AND DISCUSSION

Synthesis and characterization

The synthesis route of Oxe-PSiO modified with oxetane is shown in Scheme 1. The polyethoxylsiloxane was first synthesized via the partial hydrolysis and condensation of TEOS under the catalysis of dilute hydrochloric acid. Then the ethoxy group was substituted by oxetane group via a transetherification reaction catalyzed by titanium tetraisopropanolate. For easy understanding, the characterization for the molecular structure of Oxe-PSiO was carried out in comparison with EHO, showing the spectrum of Oxe-PSiO together with that of EHO. Figure 1 shows the ^{1}H NMR spectrum of Oxe-PSiO. The signal peak at 1.23 ppm corresponding to CH_3CH_2O—Si disappeared in the ^{1}H NMR spectrum of Oxe-PSiO. Moreover, the peak attributed to the methylene proton next to the hydroxyl group shifted from 3.78 ppm in the EHO spectrum to 3.97 ppm in the Oxe-PSiO spectrum, indicating the complete substitution of ethoxy group by oxetane group and the successful synthesis of Oxe-PSiO resin end-capped with oxetane group. From the FT-IR spectrum of Oxe-PSiO in Figure 2, it can be seen that the broad absorption

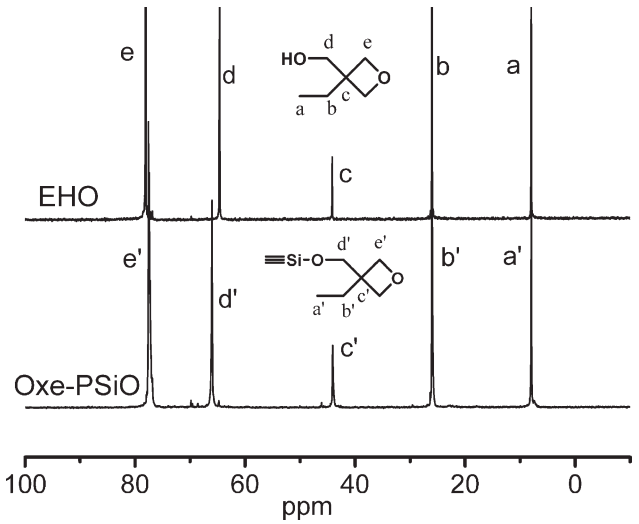

Figure 3 ^{13}C NMR spectra of EHO and Oxe-PSiO.

band from 3000 to 3700 cm^{-1} attributed to the hydroxyl group of EHO almost disappeared. While the absorption peaks at 1090 and 981 cm^{-1} are obviously observed, indicating the existence of Si—O—Si bond and oxetane group in Oxe-PSiO. Moreover, the chemical structure of Oxe-PSiO is further confirmed by ^{13}C and ^{29}Si NMR spectra. As shown in Figure 3, the signal peak attributed to the methylene carbon next to the hydroxyl group shifted from 64 ppm in the EHO spectrum to 66 ppm in the Oxe-PSiO spectrum, indicating that the oxetane group has linked to the polysiloxane resin through chemical bond. Figure 4 shows the ^{29}Si NMR spectrum of Oxe-PSiO. The Q^1, Q^2, and Q^3 peaks are attributed to the Si atoms in the end unit, linear unit, and branched unit, respectively. But no Q^4 signal peak can be observed, which was probably due to the lack of water and steric effect. This observation indicates

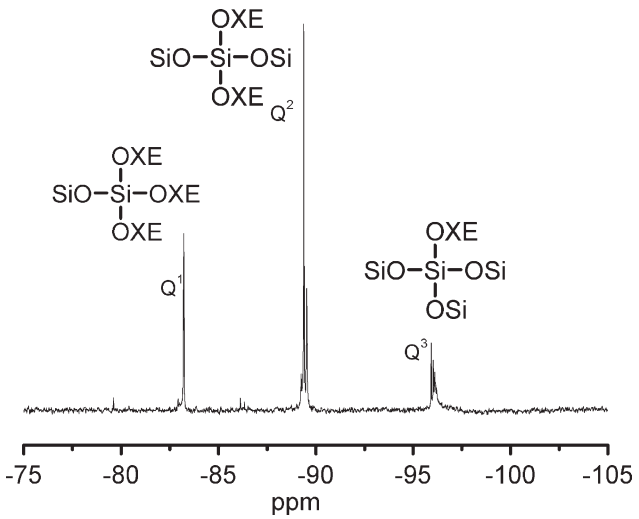

Figure 4 ^{29}Si NMR spectrum of Oxe-PSiO.

TABLE I
M_n, PDI, and Viscosity of Oxe-PSiOs

Molar ratio (water/TEOS)	M_n (g mol^{-1})	PDI	Viscosity (cps, 25°C)
0.8	1013	2.1	438
1.0	1985	1.9	12,734
1.2	2716	2.3	177,545

that both linear and branched or circular structures were formed in the silica network.

Effect of the molar ratio of water to TEOS on the molecular weight and viscosity of Oxe-PSiO

The Oxe-PSiO was synthesized based on the partial hydrolysis and condensation of TEOS in the first step. Thus the molecular weight, viscosity, and other properties of the final product were greatly affected by the molar ratio of water to TEOS. As the molar ratios of water to TEOS were set to be 0.8, 1.0, and 1.2, the different number-average molecular weights (M_ns) and polydispersity indices (PDI) were obtained by GPC to range from 1013 to 2716 g mol^{-1} and around 2.0, as listed in Table I. As more water was introduced, more ethoxy groups were hydrolyzed and condensed, directly resulting in the formation of Oxe-PSiO with higher M_n. However, when the molar ratio of water to TEOS exceeded 1.2, the synthesized Oxe-PSiO showed poor storage stability and even gelling during the synthesis process. This is probably due to the condensation of unreacted silanol group during storage stage, finally resulting in gelation.

The viscosity of synthesized Oxe-PSiO followed the same trend with M_n, sharply increasing along with the increase of molar ratio of water to TEOS, as listed in Table I. The viscosity of Oxe-PSiO at room temperature rapidly increases from 438 to 177,545 cps as the molar ratio of water to TEOS increases from 0.8 to 1.2. This can be explained that the intermolecular force becomes much stronger for the Oxe-PSiO with higher M_n, leading to the sharp increase in viscosity.

The Oxe-PSiO prepared with the water/TEOS molar ratio of 1.0 was chosen as a representative for investigating the properties in latter discussion.

Effect of Oxe-PSiO on the viscosity of UV curable formulation

The formulation viscosity directly affects the processability, leveling property, and photopolymeriaztion kinetics. Thus it is considered as one of the most important parameters, especially for UV curable systems in which no dilution solvents are applied. As listed in Table II, the viscosity of

TABLE II
Composition, Viscosity, and Photopolymerization Parameters of the DE/Oxe-PSiO Formulations

Sample	Composition (wt %) DOX	EHO	Oxe-PSiO	Viscosity (cps, 25°C)	R_{max}^{p} (J g^{-1} s^{-1})	P^{f} (%)
$DE_{100}PSiO_0$	60	40	0	17	29.5	86
$DE_{90}PSiO_{10}$	54	36	10	42	22.3	83
$DE_{70}PSiO_{30}$	42	28	30	84	20.1	79
$DE_{50}PSiO_{50}$	30	20	50	218	14.9	79

formulations with different Oxe-PSiO contents at room temperature determined by means of a rheometer increases along with the increase of Oxe-PSiO loading. Even with a 10 wt % Oxe-PSiO addition, the viscosity increases over two times compared with that of pure DE resin. The viscosity of the formulation with 50 wt % Oxe-PSiO addition increases to 218 cps from 17 cps of the pure DE resin. This can be attributed to the macromolecular structure of Oxe-PSiO, which results in a strong intermolecular force forming between DE resin and Oxe-PSiO.

Effect of Oxe-PSiO on the photopolymerization behavior

The photopolymerization kinetics is another important parameter due to its significant influence on the properties of cured films, especially for cationic UV curing systems which usually possess lower polymerization reactivity than free radical systems. For investigating the effect of synthesized Oxe-PSiO on the photopolymerization kinetics of oxetane-based cationic curing system, the phot-DSC method was used to determine the photopolymerization rate and final oxetane conversion in the cured film. As shown in Figure 5, the photopolymerization rates of all formulations show a steep increase at the beginning of irradiation, reaching a maximum value, and then decreasing rapidly. This indicates that all the formulations performed a rapidly curing behavior. Moreover, the photopolymerization rate at peak maximum (R_{max}^{p}) decreases with increasing Oxe-PSiO loading. This behavior can be mainly attributed to the sharp increase of formulation viscosity with increasing Oxe-PSiO content, which results in the restriction of motion of formed polymeric active center and previously gelling. As shown in Figure 6, the final oxetane conversion (P^{f}) in the cured films followed the same trend with R_{max}^{p}, decreasing from 86% of pure DE film to 79% of that with 50 wt % Oxe-PSiO loading.

Dynamic mechanical thermal properties

The dynamic mechanical thermal analysis (DMTA) was utilized to investigate the viscoelastic property and further examine the microstructures of cured DE/Oxe-PSiO films. The storage modulus and loss factor (tan δ) curves versus temperature are shown in Figure 7, and the detailed data are listed in Table III. The crosslinking density (V_e) is the molar number of elastically effective network chain

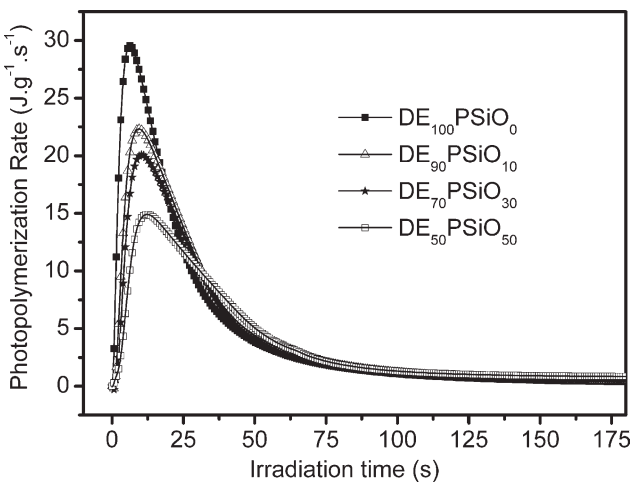

Figure 5 Photopolymerization rate of the formulations with different Oxe-PSiO contents.

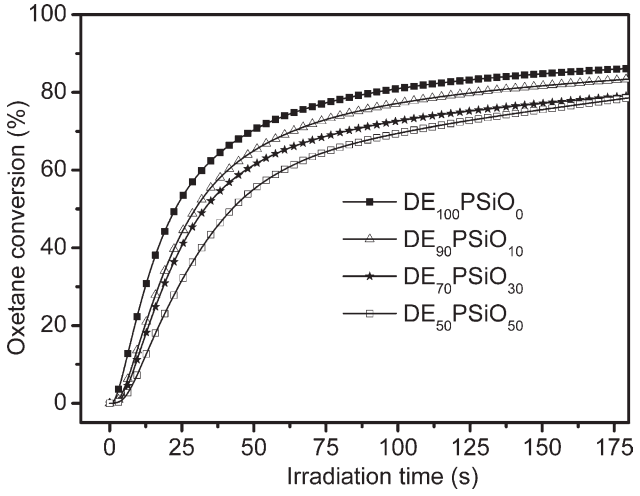

Figure 6 Oxetane conversion in the cured films with different Oxe-PSiO contents.

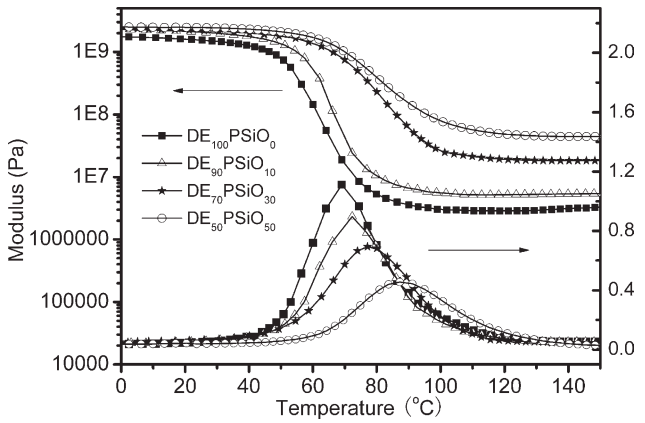

Figure 7 DMTA curves of the cured DE/Oxe-PSiO films with different Oxe-PSiO contents.

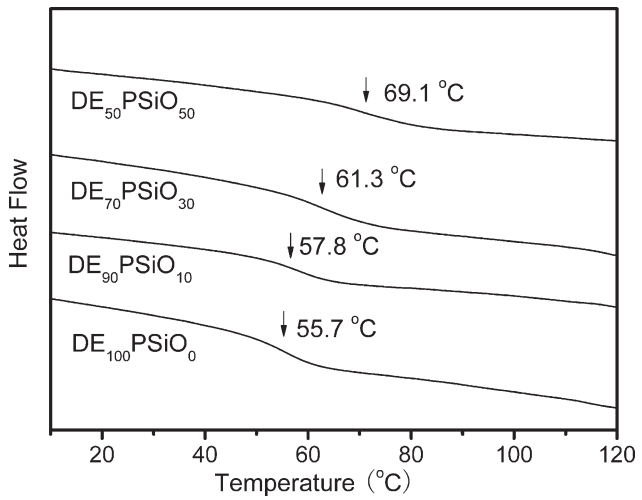

Figure 8 DSC curves of the cured DE/Oxe-PSiO films with different Oxe-PSiO contents.

per cube centimeter of cured film and can be calculated according to the formula: $V_e = E'/3RT$, where E' is the storage modulus in the rubbery state, R is the ideal gas constant, and T is the temperature at $T_g + 50$.[28] As shown in Figure 7, the E' increases from 3.2 MPa of the cured pure DE film to 44 MPa of that with 50 wt % Oxe-PSiO loading, indicating that the crosslinking density increases from 0.54 mmol cm^{-3} of the former to 4.93 mmol cm^{-3} of the latter. This behavior can be explained by the formation of silica network which restricts the segmental motion of polymeric chains and acts as a crosslinking point.

The glass transition temperature (T_g) and softening point (T_s) both follow the similar trend with E' due to the same reason as the restriction of silica network. As listed in Table III, the T_g increases from 69°C of the pure DE film to 87°C of that with 50 wt % Oxe-PSiO loading, while the T_s increases from 50 to 62°C. Moreover, the width of α relaxation peak of the loss factor which exhibits the network homogeneity can be expressed by the T_s/T_g value of cured film (Table III). All the T_s/T_g values are equal to around 0.94, indicating that the homogenous films were obtained with all formulations due to the better compatibility of Oxe-PSiO with DE resin.

The T_g of cured film was also determined by means of differential scanning calorimeter (DSC). As shown in Figure 8, the T_g increases from 55.7°C of the pure DE to 69.1°C of $DE_{50}PSiO_{50}$ due to the restriction effect of silica network on the segmental motion. In addition, the transition in the DSC curves becomes less evident along with the increase of Oxe-PSiO content, which was also observed in other hybrid systems.[29,30] However, the T_g values from DSC measurements are generally lower than those from DMTA. This phenomenon can be attributed to the frequency effect.[31]

The hardness of cured films was determined by pencil hardness tests. As shown in Table III, with the addition of 10, 30, and 50 wt % Oxe-PSiO loading, the pencil hardness of cured film increases from B to H, H and 2H, respectively. This behavior can be attributed to two factors. On the one hand, the formed silica network in the film acts as a reinforcing agent; on the other hand, the addition of polysiloxane decreases the friction coefficient of film surface, which counteracts the scratch of pencil. In addition, the increase in pencil hardness implies the improvement of scratch resistance of the cured film.

Thermal degradation behavior

The weight loss curves versus temperature measured by thermogravimetric analysis (TGA) are shown in Figure 9. The temperatures for the 10 wt % ($T_{10\%}$) and 50 wt % ($T_{50\%}$) loss and final char yield

TABLE III
Viscoelastic and Physical Properties of the Cured DE/Oxe-PSiO Films with Different Oxe-PSiO Contents

Sample	T_s (°C)	T_g (DMTA, °C)	T_s/T_g	V_e (mmol cm^{-3})	T_g (DSC, °C)	Pencil hardness
$DE_{100}PSiO_0$	50	69	0.94	0.54	55.7	B
$DE_{90}PSiO_{10}$	56	72	0.95	0.62	57.8	H
$DE_{70}PSiO_{30}$	61	77	0.95	2.09	61.3	H
$DE_{50}PSiO_{50}$	62	87	0.93	4.93	69.1	2H

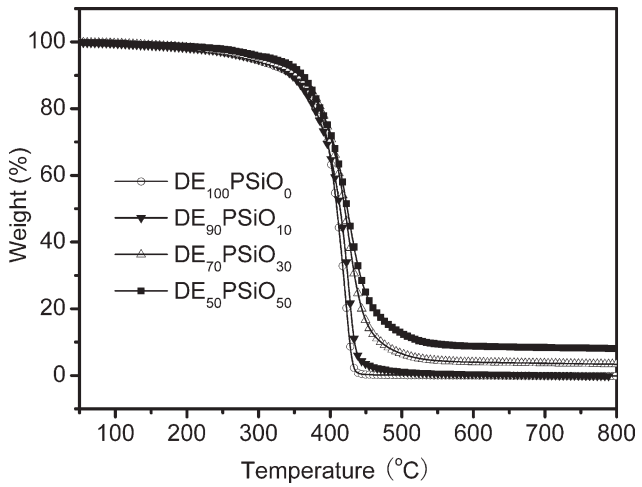

Figure 9 TGA curves of the cured DE/Oxe-PSiO films with different Oxe-PSiO contents.

are listed in Table IV. All the samples exhibit a similar thermal degradation behavior and were thermally degraded in one step, which is probably due to the decomposition of crosslinking network. However, both the $T_{10\%}$ and $T_{50\%}$ increase with increasing Oxe-PSiO loading, indicating that the thermal degradation performance of cured DE/Oxe-PSiO films is improved by the addition of Oxe-PSiO. After adding 50 wt % Oxe-PSiO the $T_{10\%}$ increases from 349°C of pure DE to 361°C, while the $T_{50\%}$ increases from 409 to 424°C. This phenomenon can be attributed to the incorporation of Si—O bond, which is one of the most thermally stable bonds due to its high bond dissociation energy, and the formation of silica network, which increases the crosslinking density. Moreover, the final char yield at 800°C also increases with increasing Oxe-PSiO content. For 50 wt % Oxe-PSiO addition, the cured film shows a char yield increase of 8.2% in comparison with the pure polymer network.

CONCLUSIONS

The oxetane-modified polysiloxanes (Oxe-PSiO) with different molecular weights were synthesized via the partial hydrolysis and condensation of TEOS, and then transetherification reaction with 3-ethyl-3-(hydroxymethyl)oxetane. Both the number-average molecular weights and viscosity of Oxe-PSiOs increase with increasing the molar ratio of water to TEOS used in hydrolyzation. The Oxe-PSiO was mixed with a commercial oxetane-based resin in different ratios to obtain a series of cationic UV curable formulations. The photo-DSC results showed that both the maximum photopolymerization rate and final oxetane conversion in the cured film decreased with the Oxe-PSiO content increasing due to the sharp increase in the formulation viscosity. The DMTA and DSC results indicated the improvement in thermal stability, showing higher T_g due to the better compatibility of Oxe-PSiO with DE resin. In addition, the greatly increased crosslinking density resulted in the enhancement of pencil hardness of cured DE/Oxe-PSiO film. Moreover, both the weight loss temperatures and final char yields measured by TGA increased with Oxe-PSiO content increasing, which means that the thermal degradation behavior of cured film was changed by the addition of Oxe-PSiO.

TABLE IV
TGA Data of the Cured DE/Oxe-PSiO Films with Different Oxe-PSiO Contents

Sample	$T_{10\%}$ (°C)	$T_{50\%}$ (°C)	Residue (%) at 800°C
$DE_{100}PSiO_0$	349	409	0
$DE_{90}PSiO_{10}$	347	414	0
$DE_{70}PSiO_{30}$	357	420	3.5
$DE_{50}PSiO_{50}$	361	424	8.2

References

1. Abe, Y.; Gunji, T. Prog Polym Sci 2004, 29, 149.
2. Majumdar, P.; Lee, E.; Gubbins, N.; Stafslien, S. J.; Daniels, J.; Thorson, C. J.; Chisholm, B. J. Polymer 2009, 50, 1124.
3. Bai, C. Y.; Zhang, X. Y.; Dai, J. B. Prog Org Coat 2007, 60, 63.
4. Vazquez, C. P.; Tayouo, R.; Joly-Duhamel, C.; Boutevin, B. J Polym Sci A Polym Chem 2010, 48, 2123.
5. Finzel, W. A.; Vincent, H. L. Federation of Societies for Coat Technology; Blue Bell: USA, 1996.
6. Diaz, I.; Chico, B.; de la Fuente, D.; Simancas, J.; Vega, J. M.; Morcillo, M. Prog Org Coat 2010, 69, 278.
7. Ogawa, T.; Watanabe, J.; Eguchi, K.; Oshima, Y. Polymer 2010, 51, 2836.
8. Schwalm, R. UV Coatings: Basics, Recent Developments and New Applications, 1st ed.; Elsevier: Amsterdam, 2007.
9. Karatas, S.; Hosgor, Z.; Kayaman-Apohan, N.; Gungor, A. Prog Org Coat 2009, 65, 49.
10. Decker, C. Macromol Rapid Commun 2002, 23, 1067.
11. Pappas, S. P., Ed. Radiation Curing, Science and Technology; Plenum Press: New York, 1992.
12. Yagci, Y.; Jockusch, S.; Turro, N. J. Macromolecules 2010, 43, 6245.
13. Decker, C.; Keller, L.; Zahouily, K.; Benfarhi, S. Polymer 2005, 46, 6640.
14. Croutxe-Barghorn, C.; Soppera, O.; Christiane, C. J Sol-Gel Sci Technol 2007, 41, 93.
15. Gigant, K.; Posset, U.; Schottner, G. J Sol-Gel Sci Technol 2003, 26, 369.
16. Soppera, O.; Croutxe-Barghorn, C. J Polym Sci A Polym Chem 2003, 41, 831.
17. Xu, J. W.; Pang, W. M.; Shi, W. F. Thin Solid Films 2006, 514, 69.
18. Malucelli, G.; Bongiovanni, R.; Sangermano, M.; Ronchetti, S.; Priola, A. Polymer 2007, 48, 7000.
19. Sangermano, M.; Bongiovanni, R.; Malucelli, G.; Priola, A.; Olbrych, J.; Harden, A. J Polym Sci A Polym Chem 2004, 42, 1415.
20. Chen, Z. G.; Zhang, Y.; Chisholm, B. J.; Webster, D. C. J Polym Sci A Polym Chem 2008, 46, 4344.

21. Versace, D.-L.; Chemtob, A.; Croutxe-Barghorn, C.; Rigolet, S. Marcromol Mater Eng 2010, 295, 355.
22. Brusatin, G.; Della Giustina, G.; Guglielmi, M.; Innocenzi, P. Prog Solid State Chem 2006, 34, 223.
23. Crivello, J. V.; Mao, Z. Chem Mater 1997, 7, 1554.
24. Crivello, J. V.; Song, K. Y.; Ghoshal, R. Chem Mater 2001, 13, 1932.
25. Sasaki, H.; Rudzinski, J. M.; Kakuchi, T. J Polym Sci A Polym Chem 1995, 33, 1807.
26. Crivello, J. V.; Sasaki, H. J Macromol Sci Pure Appl Chem 1993, A30, 189.
27. Sangermano, M.; Bongiovanni, R.; Malucelli, G.; Priola, A, Thomas, R. R.; Medsker, R. E.; Kim, Y.; Kausch, C. M. Polymer 2004, 45, 2133.
28. Masashi Kaji, K. N. T. E. J Appl Polym Sci 1999, 74, 690.
29. Hajji, P.; David, L.; Gerard, J. F.; Pascault, J. P.; Vigier, G. J Polym Sci B Polym Phys 1999, 37, 3172.
30. Motomatsu, M.; Takahashi, T.; Nie, H. Y.; Mizutani, W.; Tokumoto, H. Polymer 1997, 38, 177.
31. Nielsen, L. E. Mechanical Properties of Polymers and Composites; Marcel Dekker: New York, 1994.